Downregulation of ceramide synthase 1 promotes oral cancer through endoplasmic reticulum stress

WEN CHEN
Sichuan University West China College of Stomatology
ZHE LIU
Sichuan University West China College of Stomatology
CHENZHOU WU
Sichuan University West China College of Stomatology
YAFEI CHEN
Sichuan University West China College of Stomatology
LING QIU
Sichuan University West China College of Stomatology
ZHUOYUAN ZHANG
Sichuan University West China College of Stomatology
HAIBIN SUN
Beijing Stomatological Hospital
SIYU CHEN
Sichuan University West China College of Stomatology
ZIJIAN AN
Sichuan University West China College of Stomatology
YI LI
Sichuan University West China College of Stomatology
LONGJIANG LI (lilongjiang63@163.com)

Research

Keywords: CERS1, OSCC, ER stress, VEGFA, drug resistance

Posted Date: May 23rd, 2020

DOI: https://doi.org/10.21203/rs.3.rs-30019/v1

Version of Record: A version of this preprint was published at International Journal of Oral Science on March 22nd, 2021. See the published version at https://doi.org/10.1038/s41368-021-00118-4.

Abstract

Background

C18 ceramide (CER) plays an important role in the occurrence and development of oral squamous cell carcinoma (OSCC). However, the function of ceramide synthase 1 (CERS1), a key enzyme in C18 CER synthesis, in OSCC is still unclear. The aim of our study was to investigate the relationship between CERS1 and oral cancer.

Methods

The expression of CERS1 on 48 pairs of matching OSCC patients' cancer and normal tissues was determined by quantitative real-time PCR (RT-PCR). A mouse OSCC model induced by 4-nitroquinolin-1-oxide (4NQO) was established on CERS1+/+ and CERS1-/- C57BL/N6 mice. The functions of CERS1 downregulated were accessed by cell counting kit-8 method, colony formation assay, EdU DNA Proliferation in vitro Detection, wound healing test and Annexin V/PI double staining. RT-PCR, Western blot and luciferase assay were performed to explore the molecular mechanisms of CERS1.

Results

In this study, we found that the expression of CERS1 was downregulated in oral cancer tissues and cell lines. In the mouse OSCC model, CERS1 knockout was associated with the severity of oral malignant transformation. Immunohistochemical studies showed significant upregulation of PCNA, MMP2, MMP9, and BCL2 expression and downregulation of BAX expression in the pathological hyperplastic area. In addition, CERS1 knockdown promoted cell proliferation, migration and invasion in vitro. CERS1 knockdown caused endoplasmic reticulum stress (ER stress) and induced the activating transcription factor 4 (ATF4) pathway. ATF4 upregulated VEGFA transcription to promote tumor growth and metastasis. In addition, mild ER stress caused by CERS1 knockdown could induce cisplatin resistance.

Conclusions

Our study suggests that CERS1 is downregulated in oral cancer. The downregulation of CERS1 promotes the aggressiveness of OSCC and chemotherapeutic drug resistance by inducing mild ER stress.

Background

Oral cancer is one of the most common malignant tumors in the head and neck region, and oral squamous cell carcinoma (OSCC) is the most common pathological type of oral cancer[(1)]. Approximately one hundred thousand new OSCC patients are diagnosed worldwide every year[(2)]. The main treatment for

OSCC is combination therapy, including surgery, radiotherapy and chemotherapy. The 5-year survival rate of early-stage patients is approximately 55%-60%, while the rate of late-stage patients is only 30%-40%[3, 4]. The overall survival of OSCC patients has not changed significantly in the last few decades[5]. Therefore, it is necessary to analyze the molecular mechanisms of the development of oral cancer and strive for a new breakthrough in the study of OSCC diagnosis and treatment.

Ceramide (CER) is a kind of sphingolipid with hydrophobic chains that participates in multiple physiological functions. CER is synthesized by six different ceramide synthases (CERS). CERS are located on the endoplasmic reticulum (ER) and are necessary for the synthesis of CER. Each CERS has different selectivity for the synthesis of endogenous CER with different fatty acid chain lengths[6]. Treatment with exogenous CER promoted differentiation and inhibited proliferation in a squamous cell carcinoma cell line[7]. In addition, the function of CERS in tumors has been increasingly studied in recent years. CERS can regulate cell apoptosis, cell cycle arrest, and cell senescence.

Previous studies have demonstrated that in OSCC, CERS are involved in the regulation of apoptosis[8], EGF receptor modulation, inhibition of neovascularization[9], and enhancement of the anticancer actions of chemotherapy agents[10]. More importantly, Karahatay's study showed that decreased levels of C18 CER play important roles in the pathogenesis of OSCC[11]. Exogenous C18 CER treatment can cause tumor cell growth inhibition through a mechanism that involves the modulation of telomerase activity and induction of apoptotic cell death by mitochondrial dysfunction[12]. C18 CER is mainly synthesized by CERS1. However, the function of CERS1 in OSCC is still unknown and needs to be determined.

In the present study, we used a transgenic mouse model and RNA interference to explore the functional role of CERS1 in OSCC both in vivo and in vitro. Our study showed that CERS1 loss of function significantly promoted OSCC occurrence and progression. CERS1 loss of function could induce endoplasmic reticulum stress (ER stress) to promote VEGFA expression and chemotherapy resistance.

Materials And Methods

Cell culture and siRNA transfection

CAL27 cells, human normal oral keratinocytes (NOK), human dysplastic oral keratinocytes (DOK), HSC-2 cells and HSC-3 cells were cultured in Dulbecco's modified Eagle's medium (DMEM) (Gibco, United States) and 10% fetal bovine serum (FBS) (Gibco, United States). SCC25 cells were cultured in Dulbecco's modified Eagle's medium/Nutrient mixture F-12 (DMEM/F12) (Gibco, United States) with 10% FBS and 400 ng/ml hydrocortisone (Solarbio, China). All cells were cultured in a 5% CO2 incubator at 37 °C. The CERS1 siRNA (GeneCopoeia, United States) target sequence was AAGGTCCTGTATGCCACCAGT. The ATF4 siRNA target sequence was CUGCUUACGUUGCCAUGAU. For control siRNA, the negative control siRNA from GeneCopoeia was used. CAL27 and SCC25 cells (6×10^5-8×10^5) seeded in 6-well plates (Corning, United States) were transfected with 100 nM of each siRNA using Lipo2000 (Thermo Fisher,

United States) and FBS-free medium. After eight hours of transfection, the medium was replaced with fresh FBS-containing medium. Cells were collected 48 hours later.

Cell proliferation assay

The cell counting kit-8 method (Dojindo, China) was used to determine cell proliferation and viability. CAL27 and SCC25 cells (5×10^3) were plated in 96-well plates. After siRNA transfection, cells were incubated with 10% CCK-8 for an hour. Then, we used 480 λ to evaluate proliferation (microplate spectrophotometer, Sigma, United States).

The colony formation assay was also used to determine cell proliferation and viability. CAL27 and SCC25 cells (1×10^3) were seeded in 6-well plates. After 10 days of growth, cells were fixed with 4% paraformaldehyde (Solarbio, China) for 20 minutes and stained with 0.2% crystal violet (Solarbio, China) for 5 minutes.

EdU DNA Proliferation in vitro Detection (GeneCopoeia, United States) was used to evaluate cell proliferation. Ten micromolar EdU in DMEM was used for CAL27 and SCC25 cells in 48-well plates (3×10^4) for 2 hours. After fixation and membrane permeabilization, iClick reaction buffer was used to detect EdU. Then, the cells were stained with DAPI (Solarbio, China) for 5 minutes. A Leica microscope was used for imaging (495 nm, 360 nm) and analysis.

Cell migration and invasion assays

A wound healing test was used to test cell migration ability. CAL27 and SCC25 cells (1.5×10^6) were seeded in 6-well plates. After cell adherence, we used 200 μl pipette tips (Thermo QSP, United States) to generate wounds. A Leica microscope was used for imaging at 0 and 48 hours.

Cell invasion was tested by transwell invasion experiments. CAL27 and SCC25 cells (5×10^4) were plated in Matrigel-coated transwell chambers (Corning, 8 μm) and cultured overnight. Then, the medium in the upper chamber was changed to FBS-free medium. The medium in the lower chamber was changed to 20% FBS medium. Twenty-four hours later, the cells that had moved across the membrane were fixed, permeabilized and counted by DAPI (Servicebio) staining. A Leica microscope was used for imaging (360 nm).

Apoptosis assay

Annexin V/PI double staining (GeneCopoeia, United States) was used for apoptosis detection. CAL27 and SCC25 cells (1×10^6) were collected. After labeling with Annexin V and propidine iodide, fluorescent dye solution was added to the cells away from light for 20 minutes. Then, flow cytometry (Beckman) was used for testing (488 λ and 560 λ), and FlowJo VX was used for calculation and analysis.

Patients’ samples

Human cancer tissues and para-cancer (> 1.5 cm from the tumor margin) normal tissues were collected from 48 OSCC patients in West China hospital of Stomatology, Sichuan University (China). After resection, the tissues were immediately frozen by liquid nitrogen and stored at − 80◦C for quantitative real-time PCR (RT-PCR). Written informed consent were signed by the patients. This study was approved by the Institutional Ethical Committee of West China hospital of Stomatology (WCHSIRB-OT-2016-047).

Animal study

Both wild-type (CERS1+/+) and CERS1 knockout (CERS1-/-) C57BL/N6 mice were obtained from VITALSTAR (Beijing, China). The animals were housed in specific pathogen-free units at 24 ± 2 °C with 40-60% humidity in a 14-hour light/10-hour dark cycle with freely accessible food at Sichuan University Animal Center (Chengdu, China). Six- to eight-week-old female mice (CERS1+/+ C57BL/N6 mice, n = 25 and CERS1-/- C57BL/N6 mice, n = 25) were used for the experiments. A stock solution of 4NQO (Sigma, United States) was prepared at 5 mg/ml (in propylene glycol). Two milliliters of stock solution was added to 100 ml of double distilled water to obtain a working concentration of 100 μg/ml. The mice were treated with 4NQO for 16 weeks and then observed for another 8 weeks. At the end of the experimental period, mice were sacrificed. Tongues were collected and then longitudinally bisected. The left half of the tongue was immediately fixed in 10% buffered formalin (Solarbio, China). The right half of the tongue was immediately put into RNAstore (Tiangen, China) and stored at − 80 °C for RT-PCR. All animal experiments were approved by the Subcommittee on Research and Animal Care of Sichuan University (WCHSIRB-D-2017-227).

Histopathological analysis

Tongue tissues from the CERS1-/- group and CERS1+/+ group were processed for hematoxylin and eosin (H&E) staining. After 24 hours of fixation in 10% buffered formalin at room temperature, the tongue tissues were embedded with paraffin. After paraffin sectioning, deparaffinization and rehydration, the sections (4 μm) were stained with H&E (Solarbio, China). Histopathological diagnosis was performed by two experienced oral pathologists in a blinded manner. The tissues were classified into four types: normal epithelium, mild-moderate dysplasia, severe dysplasia/carcinoma in situ, and carcinoma.

Immunohistochemical methods were used on sections (4 μm) of tongue tissues from hyperplastic lesions. The different groups of tongue tissues were deparaffinized and rehydrated in a graded ethanol series and distilled water. The slides were immersed in 0.01 M sodium citrate buffer (pH 6.0) and heated in a water bath at 95 °C for 30 minutes. Activities of endogenous peroxidases were inhibited by using 3% hydrogen peroxide. The sections were blocked with 3% BSA (Solarbio, China) for 20 minutes. Then, the sections were incubated overnight at 4 °C with anti-BAX antibody (1:1000), anti-BCL2 antibody (1:100), anti-MMP2 antibody (1:1000), anti-MMP9 antibody (1:800), anti-PCNA antibody (1:500) and anti-VEGFA antibody (1:500). All antibodies for immunohistochemistry were from Servicebio (China).The slides were rinsed with PBS 3 times and incubated with biotinylated anti-mouse/rabbit IgG (Servicebio, China) for 50 minutes at room temperature. Then, we used diaminobenzidine to visualize the slices. Finally, nuclei were

counterstained with hematoxylin for 3 minutes at room temperature. PBS was used as a negative control instead of the primary antibody.

Five high power (40x) fields of each slides were randomly selected and evaluated under a light microscope (Leica, Germany). The assessment of IHC staining was performed by evaluating the staining intensity and the percentage of positive cells. The intensity was graded as 0 (no staining), 1 (mild staining), 2 (moderate staining), or 3 (strong staining). The proportion of stained cells was graded as 0 (negative), 1 (0-10% positive), 2 (10-30% positive) or 3 (> 30% positive). The index score ranged from 0 to 9.$\mathrm{Indexscore} = \mathrm{percentageofstaining} \times \mathrm{stainingintensity}$

Western blot

After treatment with siRNA, cells were collected, extracted with RIPA buffer (Beyotime, China) and boiled at 100 °C for 10 minutes. Then, the proteins were separated by sodium dodecyl sulfate polyacrylamide gel electrophoresis (SDS-PAGE) (10%, Bio-Rad, China) and transferred to PVDF membranes (0.22 μm, Millipore). After blocking with 5% BSA, the membrane was incubated with the primary antibody and then secondary antibody. Equivalent protein loading was confirmed using anti-GAPDH (#2118, Cell Signaling Technology, United States). Anti-CERS1 (#ab98062, Abcam, United States), anti-ATF4 (#11815, Cell Signaling Technology, United States), anti-VEGFA (#ab46154, Abcam, United States), anti-BIP (#ER40402, Huabio, China), anti-CHOP (#5554, Cell Signaling Technology, United States), anti-BAX (#5023, Cell Signaling Technology, United States) and anti-BCL2 (#4223, Cell Signaling Technology, United States) were used. A chemifluorescence kit (Bio-Rad, China) and imaging system (Bio-Rad, China) were used for visualization of blots. ImageQuant 5.2 (GE Healthcare) was used for quantification.

RNA extraction and quantitative real-time PCR

The cells were first treated with siRNA and then collected using RNAiso Plus (Takara, United States). After 20% volume of chloroform was added, and the cells were subjected to high-speed centrifugation, RNA was present in the aqueous phase. Then, an equivalent volume of isopropyl alcohol (Solarbio, China) promotes RNA degradation. After washing with 75% ethanol and dissolving in RNase-free water, RNA was transcribed into cDNA by a RevertAid RT Kit (Thermo, United States). Primers were designed by BLAST and synthesized by Sangon Biotech. SYBR Premix Ex Taq II (Takara, United States) and ABI Q7 were used for RT-PCR.

Construction of VEGFA reporter plasmids

A 2.369 kb fragment containing a 5’ VEGFA sequence from − 2304 to + 65 relative to the transcription initiation site was amplified by PCR using Q5 High-Fidelity DNA Polymerase (NEB, United States). The forward primer with a SalI site was 5’-GATGTCGACTTGCTGGGTACCACCATGGA-3’, and the reverse primer, which had a XbaI site, was 5’-GATTCTAGACAGAGCGCTGGTGCTAGCC-3’. After digestion by QuickCut restriction endonucleases (Takara, United States), a DNA Ligation Kit (Takara, United States) was used to insert the PCR sequences into the SalI and XbaI sites of pEZX-FR01 (GeneCopoeia, United States), which

contains a Rinella luciferase (Rluc) coding sequence with a CMV promoter and a promoter-less firefly luciferase (HLuc) coding sequence.

These recombinant plasmids were transfected into DH5α cells (TSINGKE, China) and amplified in nutrition agar plate (Solarbio, China) culture with kanamycin monosulfate (50 μg/ml, Solarbio, China) to select different monoclonal bacterial colonies. Then, the selected single clones were cultured in LB medium (Solarbio, China) with kanamycin. The recombinant plasmids were purified by a plasmid extraction kit (TIANGEN, China). All plasmid constructs were verified by direct sequencing (Sangon Biotech, Chengdu). The reporter plasmid was designated pEZX-VEGFA.

Plasmid transfection and luciferase assay

CAL27 cells (3×10^4) were plated in 96-well plates. After cell attachment, cells were transfected with the pEZX-VEGFA plasmid using Lipo2000 for 12 hours. Then, transfection media was replaced with the appropriate growth media. Next, the cells were divided into 4 groups based on the different treatments: control group, siNC; ATF4 knockdown group, siATF4; CERS1 knockdown group, siCERS1; and CERS1 + ATF4 knockdown group, siCERS1 + siATF4. After transfection with siRNA, a Luc-Pair Duo-Luciferase HS Assay kit (GeneCopoeia, United States) and microplate spectrophotometer were used to determine the relative luciferase activity.

Statistical analysis

IBM SPSS Statistics 20.0 was used for data statistics and analysis. Each experiment was performed independently at least three times with similar results. Data from one representative experiment are presented. The statistical methods are noted in the figure legends. $p < 0.05$ was deemed significant.

Results

CERS1 is related to the clinicopathological features and overall survival of OSCC patients

Our previous studies found that CER plays a very important role in the occurrence and development of head and neck tumors[13]. In addition, the expression of C18 CER was significantly related to oral cancer[12]. Igarashi[14] found that different CERS members exhibited a characteristic fatty acyl-CoA preference. CERS1, a transmembrane protein of the ER, catalyzes the biosynthesis of C18 CER[15, 16]. Therefore, the expression of CERS1 might also influence oral cancer.

To test this hypothesis, 48 patients with oral cancer were followed since 2016. Cancer tissues and para-cancer normal tissues were collected. By RT-PCR, we found that the expression of CERS1 in oral cancer tissues was lower than that in normal tissues ($p < 0.001$, Fig. 1A, B, C). In addition, the patients with high CERS1 expression survived longer ($p = 0.049$, Fig. 1D). The patients with lower CERS1 expression had a higher N stage ($p = 0.085$, Table 1), T stage ($p = 0.043$, Table 1) and clinical stage ($p = 0.004$). The

expression of CERS1 in normal cells, such as NOK and DOK, was higher than that in oral cancer cells, SCC25, CAL27, HSC-2 and HSC-3 ($p < 0.05$, Fig. 1E).

Table 1
Analysis of CERS1 expression in tumor tissues of patients with OSCC

	CERS1		
Characteristics	**Low expression**	**High expression**	P **value**
Gender			
Male	14	16	0.561
Female	10	8	
Age (years)			
≤ 59	13	13	1.000
> 59	11	11	
pathogenic site			
tongue	15	16	0.769
others	9	8	
smoke			
no	13	8	0.152
yes	11	16	
alcohol consumption			
no	14	8	0.085
yes	10	16	
T stage of tumor			
I-II	14	7	0.043*
III-IV	10	17	
N stage of tumor			
N0	21	12	0.004**
N1-2	3	12	
clinical stage of tumor			
I-II	14	6	0.019*
III-IV	10	18	

Note: *, $p < 0.05$; **, $p < 0.01$; ***, $p < 0.001$.

CERS1			
Pathological grade of tumor			
I	14	17	0.376
II-III	10	7	
Note: *, p < 0.05; **, p < 0.01; ***, p < 0.001.			

CERS1 knockdown promoted oral cancer in vitro

To verify the downregulation of CERS1 by siRNA interference in SCC25 and CAL27 cells, CERS1 expression levels were determined using RT-PCR. As shown in Fig. 2A, CERS1 expression levels decreased to 35% and 42% after CERS1 knockdown.

Colony formation (Fig. 2B), CCK-8 cell counting (Fig. 2C) and EdU DNA proliferation assays (Fig. 2D) are common methods for cell proliferation detection, which showed that CERS1 knockdown promoted proliferation in vitro. In addition, CERS1 knockdown promoted cell invasion (confirmed by the transwell invasion assay, Fig. 2E) and cell migration (indicated by the wound healing test, Fig. 2F).

CERS1 knockout promoted OSCC occurrence in vivo

To elucidate the role of CERS1 in OSCC development, an experimental model of 4NQO-induced oral carcinoma was established as described previously[17]. The consumption of 4NQO-water and basal diet per mouse of each group were comparable. Based on the gross appearance of the tongue, a number of mice with obvious precancerous and cancerous lesions developed in the CERS1-/- group, and the number was significantly higher than that in the CERS1+/+ group ($p < 0.05$). A total of 88% (22/25) of mice in the CERS1-/- group showed oral lesions compared with 64% (16/25) of mice in the CERS1+/+ group (Fig. 3A). The average tumor lesion size in the CERS1-/- group was 7.82 ± 7.69 mm^2. However, the average tumor lesion size in the CERS1+/+ group was smaller at 3.5 ± 5.6 mm^2 ($p = 0.033$, Fig. 3B). In addition, the number of lesions per mouse in the CERS1-/- group was significantly lower than that in the CERS1+/+ group (2.23 ± 1.02 vs. 1.88 ± 0.72, $p = 0.017$, Fig. 3C). The results showed that knocking out CERS1 contributed to the formation of tongue lesions induced by 4NQO.

Histological examination of tongue tissues was conducted by two trained pathologists blinded to the sample identities. H&E staining showed that after treatment with 4NQO, the CERS1-/- mice exhibited different stages of oral carcinogenesis than the CERS1+/+ mice. All samples were divided into four groups: normal epithelium, mild-moderate dysplasia, severe dysplasia/carcinoma in situ, and carcinoma (Fig. 3D). The results of the histopathological analysis of the CERS1-/- group and CERS1+/+ group are shown in Table 2. A total of 36% (9/25) of mice in the CERS1-/- group developed tongue squamous cell carcinoma compared with 12% (3/25) of mice in the CERS1+/+ group. These results indicated that CERS1 knockout enhanced 4NQO-induced tongue carcinogenesis.

Table 2
Histopathological examination of tongue lesions

	Mouse number	Mildmoderate Dysplasia	Severe Dysplasia or Carcinoma in Situ	Carcinoma	*P*
CERS1+/+ Group	25	19 (76%)	3 (12%)	3 (12%)	0.001
CERS1-/- Group	25	6 (24%)	10 (40%)	9 (36%)	

Proliferating cell nuclear antigen (PCNA) is only present in normal proliferating cells and tumor cells and is closely related to the synthesis of DNA[18]. It plays an important role in cell proliferation and is the key protein of abnormal cell proliferation[19]. Immunohistochemical analysis demonstrated that PCNA was mainly expressed in the nucleus. By semiquantitative assessment of IHC staining, the rate of positive nuclear PCNA expression was found to be markedly high in the CERS1-/- group ($p < 0.05$, Fig. 3E, F).

Matrix metalloproteinase-2 (MMP2) [20]and matrix metalloproteinase-9 (MMP9)[21] are important proteolytic enzymes that hydrolyze extracellular matrix and participate in the process of tumor growth and metastasis. To investigate cell invasiveness, MMP2 and MMP9 expression was assessed by immunohistochemistry. MMP2 and MMP9 were located in the cytoplasm. In the CERS1-/- group, high cytoplasmic expression of MMP2 and MMP9 was observed ($p < 0.05$, Fig. 3E, F).

BAX, a member of the BCL2 family, is a core regulator of the intrinsic apoptosis pathway[22]. BAX can affect the permeability of the outer mitochondrial membrane and subsequent initiation of the caspase cascade, which is considered a key step in apoptosis[23]. The association of BAX with BCL2 has been demonstrated through coimmunoprecipitation assays[24]. Immunohistochemistry results revealed that BAX and BCL2 were localized predominantly in the cytoplasm. The expression levels of BAX in the CERS1-/- group were lower than those in the CERS1+/+ group ($p < 0.05$, Fig. 3E, F). In contrast, the expression of BCL2 was higher ($p < 0.05$, Fig. 3E, F).

CERS1 knockdown increased VEGFA expression by ER stress

The ER is an important organelle for protein synthesis, folding and secretion in eukaryotic cells. ER stress is a kind of cellular stress state caused by protein folding dysfunction of the endoplasmic reticulum that is induced endogenously or exogenously. The expression of ER stress markers, including binding immunoglobulin protein (BIP), ATF4 and C/EBP homologous protein (CHOP), was tested by RT-PCR and Western blot. BIP is a very important molecular chaperone in ER stress that can preferentially bind to misfolded proteins in the ER. The expression of BIP in CERS1 knockdown cells was higher than that in the control group ($p < 0.05$, Fig. 4A). ATF4 is involved in the regulation of many biological processes and plays an important role in ER stress[25]. ATF4 was significantly upregulated after CERS1 knockdown ($p < 0.05$, Fig. 4A, B). ATF4 can bind to the CHOP promoter under ER stress conditions and induce the transcription of CHOP and related genes to promote the correct folding or degradation of residual

proteins[26]. Consistent with the expression of other ER stress markers, CHOP was also highly expressed in CERS1 knockdown cells ($p < 0.05$, Fig. 4A). RT-PCR of mouse lesion tongue tissues showed the same results ($p < 0.05$, Fig. 4C).

Angiogenesis is a necessary process for tumor growth, invasion and metastasis[27]. Angiogenesis refers to the formation of new abnormal blood vessels in tumors, which provide nutrition and oxygen for tumor growth. Moreover, tumor cells secrete blood vessel growth promoting factor, which positively regulates this process[28]. Vascular endothelial growth factor A (VEGFA) is an effective endothelial cell-specific regulator of angiogenesis that influences tumor growth and metastasis[29]. It has been shown that ATF4 can regulate VEGFA transcription under ER stress in cancer cells[30]. Our results found that VEGFA was located in the cytoplasm in mouse tongue specimens. Strong expression of VEGFA was observed in the CERS1-/- group mice ($p < 0.05$ Fig. 4C, D). In addition, we found that VEGFA expression was higher in CERS1 knockdown cells in vitro ($p < 0.05$, Fig. 4A, B).

To prove that CERS1 knockdown led to increased VEGFA expression through ATF4, we used a luciferase reporter plasmid in which a VEGFA 5'-flanking sequence (-2304 to + 65 relative to the transcription initiation site) was fused to the firefly luciferase coding sequences in the pEZX-FR01 vector. The Renilla luciferase in the plasmid had its own replication origin (SV40), which was used as an internal control. The pEZX-VEGFA (Fig. 4E) plasmid was cotransfected into CAL27 cells with different siRNAs. The activities of both firefly luciferase and Renilla luciferase were measured using the dual luciferase assay. As shown in Fig. 4E, a low level of VEGFA promoter activity was detected in ATF4 knockdown cells, whereas a high level of VEGFA promoter activity was detected in CERS1 knockdown cells. Additionally, in both ATF4 and CERS1 knockdown cells, VEGFA promoter activity was also low. These results suggested that VEGFA promoter activity is responsible for the low expression of CERS1 through ATF4 upregulation.

CERS1 knockdown led to mild ER stress causing cisplatin resistance

Cisplatin (referred to as DDP in the group name) is a first-line drug for OSCC treatment. The high incidence of drug resistance is the main limiting factor of the clinical efficacy of cisplatin[31]. Recent studies have shown that high CERS1 expression renders cells more sensitive to cisplatin[32]. As we have found that CERS1 is usually downregulated in OSCC samples (Fig. 1), we explored the relationship between CERS1 knockdown and cisplatin resistance.

A previous study showed that the ER adapts to endogenous and exogenous stressors by expanding its protein-folding capacity and by stimulating protective processes[33]. Triggering continued mild ER stress to sustain ER homeostasis is considered a treatment for some diseases[34]. Tunicamycin (TM), a UDP-N-acetylglucosamine-dolichol phosphate N-acetylglucosamine-1-phosphate transferase inhibitor, can block the initial step of glycoprotein biosynthesis in the ER. TM is now well known as a classical ER stress inducer[35]. Mild ER stress can be induced by treating cells with low-dose TM (1 μg/ml, Sigma) for 2 hours, which was used as a positive control.

There were 4 groups in the experiment that underwent various treatments as follows: siNC group, transfected with NC siRNA and treated with 1% DMSO; siNC + DDP group, transfected with NC siRNA and treated with cisplatin (40 nM, Sigma) for 12 hours; siNC + TM + DDP group, transfected with NC siRNA, pretreated with TM (1 μg/ml) for 2 hours and then treated with cisplatin for 12 hours; and siCERS1 + DDP group, with CERS1 knockdown and then treated with cisplatin for 12 hours. The expression of BIP, ATF4 and CHOP was higher in the siNC + TM + DDP and siCERS1 + DDP groups than in the siNC and siNC + DDP groups ($p < 0.05$, Fig. 5A, B). In addition, the annexin V/PI double staining assay showed that after treatment with cisplatin, the number of apoptotic cells in the siNC + DDP group was significantly higher than that in the siNC group ($p < 0.05$, Fig. 5C). However, after treatment with TM, the number of apoptotic cells decreased significantly. The siCERS1 + DDP group showed the same result. The expression of BAX and BCL2 showed the same results (Fig. 5A, B). These findings indicated that knockdown of CERS1 could trigger mild ER stress and induce cisplatin resistance.

Discussion

In this study, we investigated the roles and mechanisms of CERS1 in OSCC. Our data suggested that decreased levels of CERS1 might play important roles in oral cancer. CERS1 expression was lower in OSCC tissues than in controls. In addition, patients with lower expression of CERS1 in tumor tissues had a worse prognosis. Further data showed that downregulation of CERS1 resulted in the inhibition of cell apoptosis and promotion of cell proliferation and invasion, which involved the induction of mild ER stress and modulation of the protein kinase R-like endoplasmic reticulum kinase (PERK)/eukaryotic translation initiation factor 2α (eIF2α)/ATF4 pathway in OSCC. These results suggested that decreased levels of CERS1 conferred a growth advantage to cancer cells.

Our research group has performed this research with siRNA[36]-mediated CERS1 knockdown in OSCC. In addition, knockout of CERS1 in mice was used to establish a mouse model of oral carcinogenesis. 4NQO is an aromatic amine heterocyclic compound that is often used as an inducer in oral cancer animal models[37]. Oral cancer induced by the 4NQO carcinogen ranges from simple epithelial growth to invasive cancer. This process is similar to the real human disease process, making is more suitable to the capture and exploration of disease mechanisms[38]. In this study, CERS1 knockout mice were treated with 4NQO. This was also the first study to explore the effect of CERS1 on the occurrence and development of oral cancer in vivo. CERS1 knockout mice were more likely to develop oral cancer, which was consistent with the vitro experiments and other studies[39].

CERS are membrane proteins of the ER and synthesize (dihydro) CER with the N-acylation of the (dihydro) sphingosine backbone[40]. CERS1–CERS6 have been identified, each of which catalyzes different lengths of acyl chains to produce CER. CERS1 uses C18-acyl-CoA, which is related to oral cancer cell autophagic cell death[41]. CER can reduce protein kinase B (AKT) activity by activating protein phosphatase 2A (PP2A), p38[42] and protein kinase C (PKC)[43], and then AKT reduces the phosphorylation level of BCL2[42, 44]. Finally, the decreased level of BCL2 and the ratio of BCL2 to BAX leads to cell death.

Immunohistochemistry results confirmed this effect. Reducing CERS1 inhibits the synthesis of C18 CER, AKT and BCL2 to inhibit apoptosis.

The ER is an organelle widely present in eukaryotic cells that regulates protein synthesis, folding and aggregation after synthesis. An aggregation of misfolded proteins in the lumen and an imbalance of Ca2 + in the cytoplasm caused by various factors can lead to ER dysfunction, which can induce a series of related protein expression and cell phenotype changes, a condition called ER stress[45]. ER stress mainly involves three ER transmembrane effector proteins, inositol-requiring enzyme 1, PERK and activating transcription factor 6. When unfolded proteins accumulate, BIP dissociates from those proteins and binds to unfolded or misfolded proteins to help with proper folded[46]. Activated PERK further phosphorylates the downstream eIF2α, ATF4 and CHOP[47, 48]. The expression of PERK-ATF4 has been positively correlated with VEGF[49]. In our study, after knocking down/out CERS1, the expression of BIP, ATF4, CHOP and VEGFA was higher than that in the control group. VEGFA promoter activity was related to CERS1 knockdown. However, ATF4 knockdown abolished this relationship. Therefore, downregulation of CERS1 promotes migration through ER stress, the PERK-ATF4 pathway and VEGFA.

Chemotherapy is one of the main treatments for oral cancer. However, some tumors become resistant during the course of treatment, which greatly limits the efficacy. Junxia Min's research showed that CERS1 expression rendered cells more sensitive to cisplatin, carboplatin, doxorubicin, and vincristine[32]. In addition, dasatinib induces apoptosis by upregulating the expression levels of CERS1[50]. Different mechanisms of resistance to CERS1 have been investigated. However, we are far from having a full understanding of all CERS1 resistance-related pathways. As our study, CERS1 knockdown induced ER stress, which is a process that can remove misfolded proteins in the ER through the unfolded protein response to maintain ER homeostasis. If ER stress is not reversed, it will lead to cell function deterioration and cell death[51]. However, mild ER stress sustains ER homeostasis, which is an attractive strategy for cancer[52]. In our study, TM, a classical ER stress drug, was used as a positive control to explore the relationship between CERS1, mild ER stress and drug resistance. Similar to the result of low-dose TM, CERS1 knockdown caused mild ER stress and then reduce the apoptosis caused by cisplatin. Overall, downregulation of CERS1 plays a negative role in chemotherapy for oral cancer.

Conclusions

In this study, we revealed that the downregulation of CERS1 in OSCC was associated with poor prognosis. Our results also demonstrated that CERS1 knockdown significantly promoted cancer cell proliferation, invasion and migration. More importantly, we showed that downregulation of CERS1 maintained VEGFA promoter activity via the PERK-ATF4 pathway. In addition, downregulation of CERS1 induced cisplatin resistance through mild ER stress. Overall, the detection of CERS1 expression may be meaningful for guiding the OSCC clinical treatment options. CERS1 may be a promising target for OSCC treatment.

Abbreviations

CER: C18 ceramide; OSCC: oral squamous cell carcinoma; CERS1: ceramide synthase 1; RT-PCR: quantitative real-time PCR; 4NQO: 4-nitroquinolin-1-oxide; ER stress: endoplasmic reticulum stress; ATF4: activating transcription factor 4; CERS: ceramide synthases; ER: endoplasmic reticulum; NOK: human normal oral keratinocytes; DOK: human dysplastic oral keratinocytes; FBS: fetal bovine serum; Rluc: Rinella luciferase; HLuc: firefly luciferase; PCNA: proliferating cell nuclear antigen; MMP2: matrix metalloproteinase-2; MMP9: matrix metalloproteinase-9; BIP: binding immunoglobulin protein; CHOP: C/EBP homologous protein; VEGFA: vascular endothelial growth factor A; DDP: cisplatin; TM: tunicamycin; PERK: protein kinase R-like endoplasmic reticulum kinas; eIF2α: eukaryotic translation initiation factor 2α; AKT: protein kinase B; PP2A: protein phosphatase 2A; PKC: protein kinase C

Declarations

Acknowledgements

Not applicable.

Authors' contributions

WC and ZL contributed equally to this work. WC, ZL, LL conceived and designed the experiments. WC, YC, LQ, ZZ, SC and ZA performed the experiments. CW contributed clinical materials and performed the data acquisition, analysis and interpretation. LL provided technical and scientific support. WC and ZL were involved in the manuscript preparation. All authors read and approved the final manuscript.

Funding

This work was supported by National Natural Science Foundation of China [81972538].

Availability of data and materials

All data and materials supporting the conclusions of this study were included in the article.

Ethics approval and consent to participate

The study was approved by the Institutional Ethical Committee of West China hospital of Stomatology (WCHSIRB-OT-2016-047) and the Subcommittee on Research and Animal Care of Sichuan University (WCHSIRB-D-2017-227).

Consent for publication

Not applicable.

Competing interests

The authors declare that they have no competing interests

Author details

[1]State Key Laboratory of Oral Diseases & National Clinical Research Center for Oral Diseases & Department of Head and Neck Oncology, West China Hospital of Stomatology, Sichuan University, Number 14, Unit 3, Renmin Nan Road, Chengdu City, Sichuan 610041, China.

[2]Department of Oral and Maxillofacial-Head and Neck Oncology, Capital Medical University School of Stomatology, Beijing, 100050, China.

References

1. Ara SA, Ashraf S, Patil BM. Evaluation of serum uric acid levels in patients with oral squamous cell carcinoma. Indian J Dent Res. 2016;2:178–83. doi:10.4103/0970-9290.183128.
2. Bose P, Brockton NT, Dort JC. Head and neck cancer: from anatomy to biology. Int J Cancer. 2013;9:2013–23. doi:10.1002/ijc.28112.
3. Lin CS, de Oliveira Santos AB, Silva EL, de Matos LL, Moyses RA, Kulcsar MA, Pinto FR, Brandão LG, Cernea CR. Tumor volume as an independent predictive factor of worse survival in patients with oral cavity squamous cell carcinoma. Head Neck. 2017;5:960–4. doi:10.1002/hed.24714.
4. da Silva SD, Ferlito A, Takes RP, Brakenhoff RH, Valentin MD, Woolgar JA, Bradford CR, Rodrigo JP, Rinaldo A. M. P. Hier and L. P. Kowalski: Advances and applications of oral cancer basic research. Oral Oncol. 2011;9:783–91. doi:10.1016/j.oraloncology.2011.07.004.
5. Wen CP, Tsai MK, Chung WS, Hsu HL, Chang YC, Chan HT, Chiang PH, Cheng TY, Tsai SP. Cancer risks from betel quid chewing beyond oral cancer: a multiple-site carcinogen when acting with smoking. Cancer Causes Control. 2010;9:1427–35. doi:10.1007/s10552-010-9570-1.
6. Harvey DJ. Analysis of carbohydrates and glycoconjugates by matrix-assisted laser desorption/ionization mass spectrometry: an update covering the period 2001–2002. Mass Spectrom Rev. 2008;2:125–201. doi:10.1002/mas.20157.
7. Wakita H, Tokura Y, Yagi H, Nishimura K, Furukawa F, Takigawa M. Keratinocyte differentiation is induced by cell-permeant ceramides and its proliferation is promoted by sphingosine. Arch Dermatol Res. 1994;6:350–4. doi:10.1007/bf00402228.
8. Rodriguez-Lafrasse C, Alphonse G, Broquet P, Aloy MT, Louisot P, Rousson R. Temporal relationships between ceramide production, caspase activation and mitochondrial dysfunction in cell lines with varying sensitivity to anti-Fas-induced apoptosis. Biochem J. 2001;Pt 2:407–16. doi:10.1042/0264-6021:3570407.
9. Meisinger J, Patel S, Vellody K, Bergstrom R, Benefield J, Lozano Y, Young MR. Protein phosphatase-2A association with microtubules and its role in restricting the invasiveness of human head and neck squamous cell carcinoma cells. Cancer Lett. 1997;1–2:87–95. doi:10.1016/s0304-3835(96)04517-x.
10. Senkal CE, Ponnusamy S, Rossi MJ, Sundararaj K, Szulc Z, Bielawski J, Bielawska A, Meyer M, Cobanoglu B, Koybasi S, Sinha D, Day TA, Obeid LM, Hannun YA, Ogretmen B. Potent antitumor

activity of a novel cationic pyridinium-ceramide alone or in combination with gemcitabine against human head and neck squamous cell carcinomas in vitro and in vivo. J Pharmacol Exp Ther. 2006;3:1188–99. doi:10.1124/jpet.106.101949.

11. Karahatay S, Thomas K, Koybasi S, Senkal CE, Elojeimy S, Liu X, Bielawski J, Day TA, Gillespie MB, Sinha D, Norris JS, Hannun YA, Ogretmen B. Clinical relevance of ceramide metabolism in the pathogenesis of human head and neck squamous cell carcinoma (HNSCC): attenuation of C(18)-ceramide in HNSCC tumors correlates with lymphovascular invasion and nodal metastasis. Cancer Lett. 2007;1:101–11. doi:10.1016/j.canlet.2007.06.003.
12. Koybasi S, Senkal CE, Sundararaj K, Spassieva S, Bielawski J, Osta W, Day TA, Jiang JC, Jazwinski SM, Hannun YA, Obeid LM, Ogretmen B. Defects in cell growth regulation by C18:0-ceramide and longevity assurance gene 1 in human head and neck squamous cell carcinomas. J Biol Chem. 2004;43:44311–9. doi:10.1074/jbc.M406920200.
13. Qiu L, Liu Z, Wu C, Chen W, Chen Y, Zhang B, Li J, Liu H, Huang N, Jiang Z, Wu Y, Li L. C6-ceramide induces salivary adenoid cystic carcinoma cell apoptosis via IP3R-activated UPR and UPR-independent pathways. Biochem Biophys Res Commun. 2020;4:997–1003. doi:10.1016/j.bbrc.2020.02.164.
14. Mizutani Y, Kihara A, Chiba H, Tojo H, Igarashi Y. 2-Hydroxy-ceramide synthesis by ceramide synthase family: enzymatic basis for the preference of FA chain length. J Lipid Res. 2008;11:2356–64. doi:10.1194/jlr.M800158-JLR200.
15. Vanni N, Fruscione F, Ferlazzo E, Striano P, Robbiano A, Traverso M, Sander T, Falace A, Gazzerro E, Bramanti P, Bielawski J, Fassio A, Minetti C, Genton P, Zara F. Impairment of ceramide synthesis causes a novel progressive myoclonus epilepsy. Ann Neurol. 2014;2:206–12. doi:10.1002/ana.24170.
16. Ferlazzo E, Striano P, Italiano D, Calarese T, Gasparini S, Vanni N, Fruscione F, Genton P, Zara F. Autosomal recessive progressive myoclonus epilepsy due to impaired ceramide synthesis. Epileptic Disord. 2016;S2:120–7. doi:10.1684/epd.2016.0857.
17. Wu JS, Li L, Wang SS, Pang X, Wu JB, Sheng SR, Tang YJ, Tang YL, Zheng M, Liang XH. Autophagy is positively associated with the accumulation of myeloid–derived suppressor cells in 4–nitroquinoline–1–oxide–induced oral cancer. Oncol Rep. 2018;6:3381–91. doi:10.3892/or.2018.6747.
18. Masuda Y, Masutani C. Spatiotemporal regulation of PCNA ubiquitination in damage tolerance pathways. Crit Rev Biochem Mol Biol. 2019;5:418–42. doi:10.1080/10409238.2019.1687420.
19. Maga G, Hubscher U. Proliferating cell nuclear antigen (PCNA): a dancer with many partners. J Cell Sci. 2003;Pt 15: 3051–60. doi:10.1242/jcs.00653.
20. Chan OTM, Furuya H, Pagano I, Shimizu Y, Hokutan K, Dyrskjøt L, Jensen JB, Malmstrom PU, Segersten U, Janku F, Rosser CJ. Association of MMP-2, RB and PAI-1 with decreased recurrence-free survival and overall survival in bladder cancer patients. Oncotarget. 2017;59:99707–21. doi:10.18632/oncotarget.20686.

21. Gong D, Zhang J, Chen Y, Xu Y, Ma J, Hu G, Huang Y, Zheng J, Zhai W, Xue W. The m(6)A-suppressed P2RX6 activation promotes renal cancer cells migration and invasion through ATP-induced Ca(2+) influx modulating ERK1/2 phosphorylation and MMP9 signaling pathway. J Exp Clin Cancer Res. 2019;1:233. doi:10.1186/s13046-019-1223-y.
22. Edlich F. BCL-2 proteins and apoptosis: Recent insights and unknowns. Biochem Biophys Res Commun. 2018;1:26–34. doi:10.1016/j.bbrc.2017.06.190.
23. Liu L, Liu Y, Zhang T, Wu H, Lin M, Wang C, Zhan Y, Zhou Q, Qiao B, Sun X, Zhang Q, Guo X, Zhao G, Zhang W, Huang W. Synthetic Bax-Anti Bcl2 combination module actuated by super artificial hTERT promoter selectively inhibits malignant phenotypes of bladder cancer. J Exp Clin Cancer Res. 2016: 3. doi:10.1186/s13046-015-0279-6.
24. Oltvai ZN, Milliman CL, Korsmeyer SJ. Bcl-2 heterodimerizes in vivo with a conserved homolog, Bax, that accelerates programmed cell death. Cell. 1993;4:609–19. doi:10.1016/0092-8674(93)90509-o.
25. Nakamura S, Miki H, Kido S, Nakano A, Hiasa M, Oda A, Amou H, Watanabe K, Harada T, Fujii S, Takeuchi K, Kagawa K, Ozaki S, Matsumoto T, Abe M. Activating transcription factor 4, an ER stress mediator, is required for, but excessive ER stress suppresses osteoblastogenesis by bortezomib. Int J Hematol. 2013;1:66–73. doi:10.1007/s12185-013-1367-z.
26. Iida K, Li Y, McGrath BC, Frank A, Cavener DR. PERK eIF2 alpha kinase is required to regulate the viability of the exocrine pancreas in mice. BMC Cell Biol. 2007: 38. doi:10.1186/1471-2121-8-38.
27. Hanahan D, Weinberg RA. Hallmarks of cancer: the next generation. Cell. 2011;5:646–74. doi:10.1016/j.cell.2011.02.013.
28. Potente M, Gerhardt H, Carmeliet P. Basic and therapeutic aspects of angiogenesis. Cell. 2011;6:873–87. doi:10.1016/j.cell.2011.08.039.
29. Andersen S, Donnem T, Al-Shibli K, Al-Saad S, Stenvold H, Busund LT, Bremnes RM. Prognostic impacts of angiopoietins in NSCLC tumor cells and stroma: VEGF-A impact is strongly associated with Ang-2. PLoS One. 2011;5:e19773. doi:10.1371/journal.pone.0019773.
30. Ghosh R, Lipson KL, Sargent KE, Mercurio AM, Hunt JS, Ron D, Urano F. Transcriptional regulation of VEGF-A by the unfolded protein response pathway. PLoS One. 2010;3:e9575. doi:10.1371/journal.pone.0009575.
31. Chen SH, Chang JY. New Insights into Mechanisms of Cisplatin Resistance: From Tumor Cell to Microenvironment. Int J Mol Sci. 2019;17. doi:10.3390/ijms20174136.
32. Min J, Mesika A, Sivaguru M, Van Veldhoven PP, Alexander H, Futerman AH. and S. Alexander: (Dihydro)ceramide synthase 1 regulated sensitivity to cisplatin is associated with the activation of p38 mitogen-activated protein kinase and is abrogated by sphingosine kinase 1. Mol Cancer Res. 2007;8:801–12. doi:10.1158/1541-7786.mcr-07-0100.
33. Wang X, Eno CO, Altman BJ, Zhu Y, Zhao G, Olberding KE, Rathmell JC, Li C. ER stress modulates cellular metabolism. Biochem J. 2011;1:285–96. doi:10.1042/bj20101864.
34. Koc M, Mayerová V, Kračmerová J, Mairal A, Mališová L, Štich V, Langin D, Rossmeislová L. Stress of endoplasmic reticulum modulates differentiation and lipogenesis of human adipocytes. Biochem

Biophys Res Commun. 2015;3:684–90. doi:10.1016/j.bbrc.2015.03.090.

35. Oslowski CM, Urano F. Measuring ER stress and the unfolded protein response using mammalian tissue culture system. Methods Enzymol. 2011: 71–92. doi:10.1016/b978-0-12-385114-7.00004-0.
36. Senkal CE, Ponnusamy S, Rossi MJ, Bialewski J, Sinha D, Jiang JC, Jazwinski SM, Hannun YA, Ogretmen B. Role of human longevity assurance gene 1 and C18-ceramide in chemotherapy-induced cell death in human head and neck squamous cell carcinomas. Mol Cancer Ther. 2007;2:712–22. doi:10.1158/1535-7163.mct-06-0558.
37. Brüsehafer K, Manshian BB, Doherty AT, Zaïr ZM, Johnson GE, Doak SH, Jenkins GJ. The clastogenicity of 4NQO is cell-type dependent and linked to cytotoxicity, length of exposure and p53 proficiency. Mutagenesis. 2016;2:171–80. doi:10.1093/mutage/gev069.
38. der Ploeg-van den
10.1002/lsm.22197
de Visscher SA, Witjes MJ, van der Vegt B, HS de Bruijn, A. van der Ploeg-van den Heuvel A, Amelink HJ, Sterenborg JL, Roodenburg, Robinson DJ. Localization of liposomal mTHPC formulations within normal epithelium, dysplastic tissue, and carcinoma of oral epithelium in the 4NQO-carcinogenesis rat model. Lasers Surg Med. 2013;10: 668–78. doi:10.1002/lsm.22197.
39. Wang Z, Wen L, Zhu F, Wang Y, Xie Q, Chen Z, Li Y. Overexpression of ceramide synthase 1 increases C18-ceramide and leads to lethal autophagy in human glioma. Oncotarget. 2017;61:104022–36. doi:10.18632/oncotarget.21955.
40. Stiban J, Tidhar R, Futerman AH. Ceramide synthases: roles in cell physiology and signaling. Adv Exp Med Biol. 2010: 60–71. doi:10.1007/978-1-4419-6741-1_4.
41. Venkataraman K, Riebeling C, Bodennec J, Riezman H, Allegood JC, Sullards MC, Merrill AH, Futerman AH. Upstream of Growth and Differentiation Factor 1 (uog1), a Mammalian Homolog of the Yeast Longevity Assurance Gene 1 (LAG1), RegulatesN-Stearoyl-sphinganine (C18-(Dihydro)ceramide) Synthesis in a Fumonisin B1-independent Manner in Mammalian Cells. J Biol Chem. 2002;38:35642–9.
42. Kim HJ, Oh JE, Kim SW, Chun YJ, Kim MY. Ceramide induces p38 MAPK-dependent apoptosis and Bax translocation via inhibition of Akt in HL-60 cells. Cancer Lett. 2008;1–2:88–95. doi:10.1016/j.canlet.2007.10.030.
43. Bourbon NA, Sandirasegarane L, Kester M. Ceramide-induced inhibition of Akt is mediated through protein kinase Czeta: implications for growth arrest. J Biol Chem. 2002;5:3286–92. doi:10.1074/jbc.M110541200.
44. Tsuruta F, Sunayama J, Mori Y, Hattori S, Shimizu S, Tsujimoto Y, Yoshioka K, Masuyama N, Gotoh Y. JNK promotes Bax translocation to mitochondria through phosphorylation of 14-3-3 proteins. Embo j. 2004;8:1889–99. doi:10.1038/sj.emboj.7600194.
45. C. M. Dobson: Protein Folding and Misfolding. Nature. 2003;6968: 884–890.
46. Bertolotti A, Zhang Y, Hendershot LM, Harding HP, Ron D. Dynamic interaction of BiP and ER stress transducers in the unfolded-protein response. Nat Cell Biol. 2000;6:326–32. doi:10.1038/35014014.

47. Nishitoh H. CHOP is a multifunctional transcription factor in the ER stress response. J Biochem. 2012;3:217–9. doi:10.1093/jb/mvr143.
48. Harding HP, Zhang Y, Bertolotti A, Zeng H, Ron D. Perk is essential for translational regulation and cell survival during the unfolded protein response. Mol Cell. 2000;5:897–904. doi:10.1016/s1097-2765(00)80330-5.
49. Afonyushkin T, Oskolkova OV, Philippova M, Resink TJ, Erne P, Binder BR, Bochkov VN. Oxidized phospholipids regulate expression of ATF4 and VEGF in endothelial cells via NRF2-dependent mechanism: novel point of convergence between electrophilic and unfolded protein stress pathways. Arterioscler Thromb Vasc Biol. 2010;5:1007–13. doi:10.1161/atvbaha.110.204354.
50. Gencer EB, Ural AU, Avcu F, Baran Y. A novel mechanism of dasatinib-induced apoptosis in chronic myeloid leukemia; ceramide synthase and ceramide clearance genes. Ann Hematol. 2011;11:1265–75. doi:10.1007/s00277-011-1212-5.
51. Shore GC, Papa FR, Oakes SA. Signaling cell death from the endoplasmic reticulum stress response. Curr Opin Cell Biol. 2011;2:143–9. doi:10.1016/j.ceb.2010.11.003.
52. Ma M, Song L, Yan H, Liu M, Zhang L, Ma Y, Yuan J, Hu J, Ji Z, Zhang R, Li C, Wang H, Tao L, Zhang Y, Li Y. Low dose tunicamycin enhances atherosclerotic plaque stability by inducing autophagy. Biochem Pharmacol 2016: 51–60. doi:10.1016/j.bcp.2015.11.020.

Figures

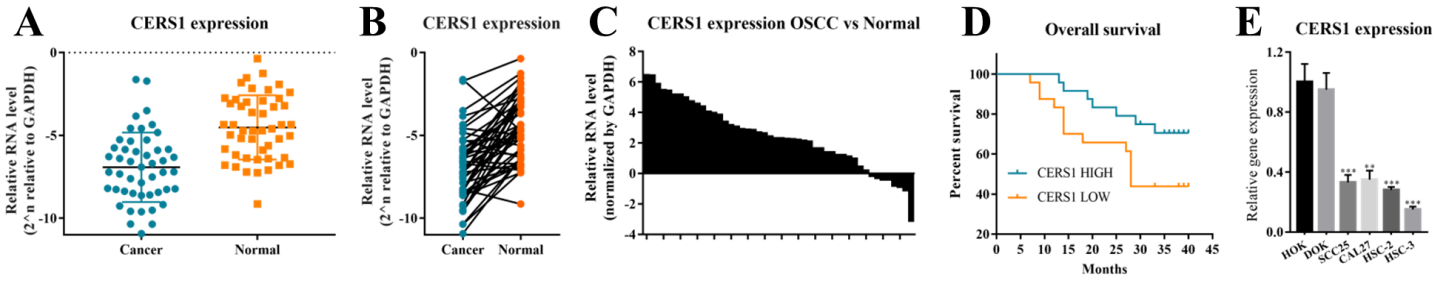

Figure 1

CERS1 correlated with OSCC and its prognosis. A, RT-PCR was used to determine the expression of CERS1 in 48 OSCC tissues and 48 normal tissues. B, RT-PCR analysis of the relative expression of CERS1 in 48 OSCC tissues and their paired adjacent normal tissues. C, RT-PCR results showed that the expression of CERS1 in OSCC tissues was higher than that in paired adjacent normal tissues. D, Kaplan–Meier survival curves showed that low CERS1 expression was associated with poor overall survival. The log-rank test was used. E, RT-PCR showed that the expression of CERS1 in OSCC cells (SCC25, CAL27, HSC-2, HSC-3) was lower than that in normal cells (NOK, DOK). For A and E, Student's t test was used. For B and C, a paired t test was used. Note: *, $p < 0.05$; **, $p < 0.01$; ***, $p < 0.001$.

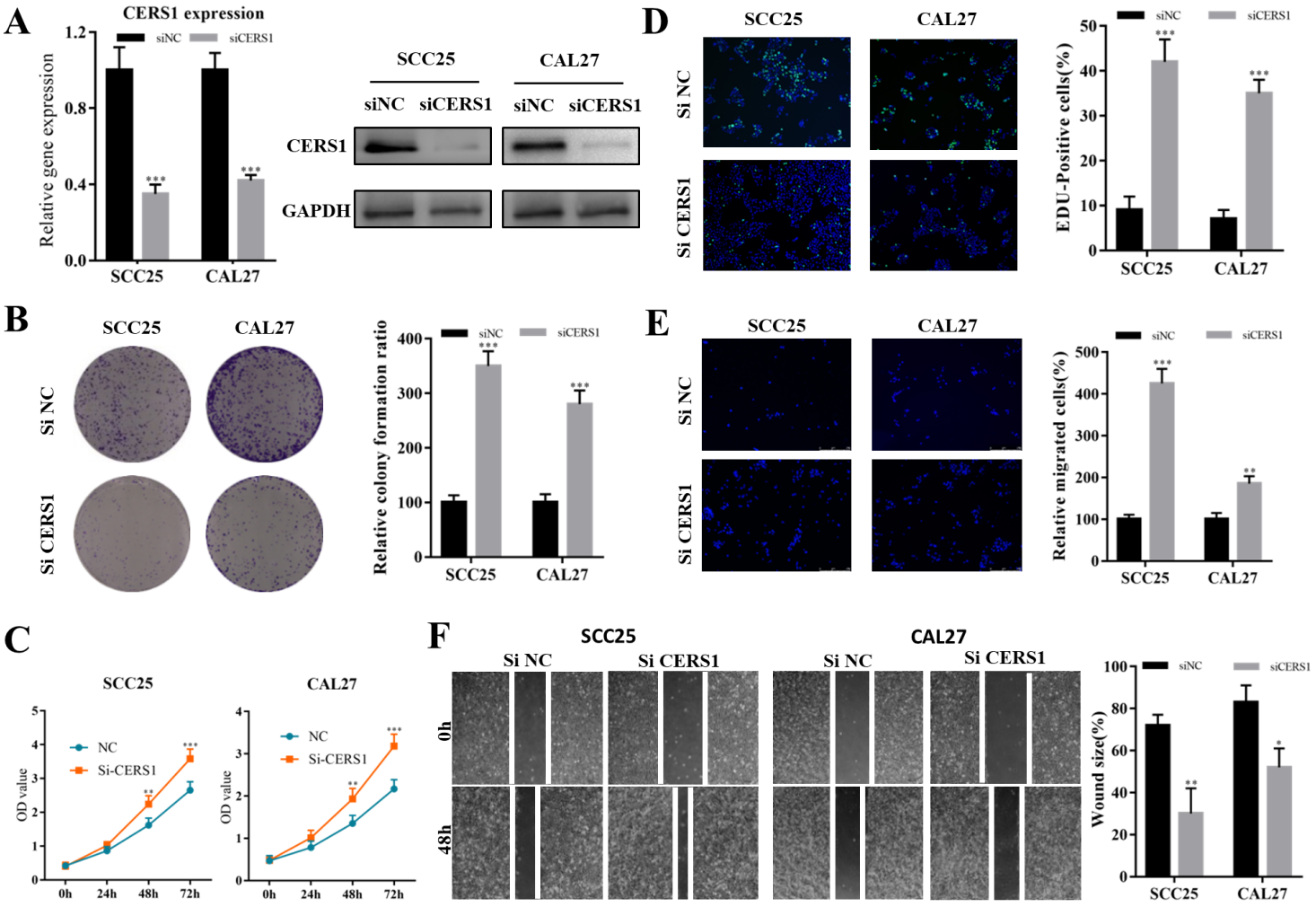

Figure 2

CERS1 knockdown promoted OSCC progression in vitro. A, RT-PCR and Western blot confirmed CERS1 knockdown. B to D, colony formation assay (B), cell counting kit-8 assay (C), and EdU DNA proliferation in vitro detection assay (D) confirmed that CERS1 knockdown promoted OSCC proliferation. E and F, transwell invasion assays (E) and wound healing tests (F) confirmed that CERS1 knockdown promoted OSCC migration and invasion ability. For A to F, Student's t test was used. For C, Student's t test was used for each time point. Note: *, $p < 0.05$; **, $p < 0.01$; ***, $p < 0.001$.

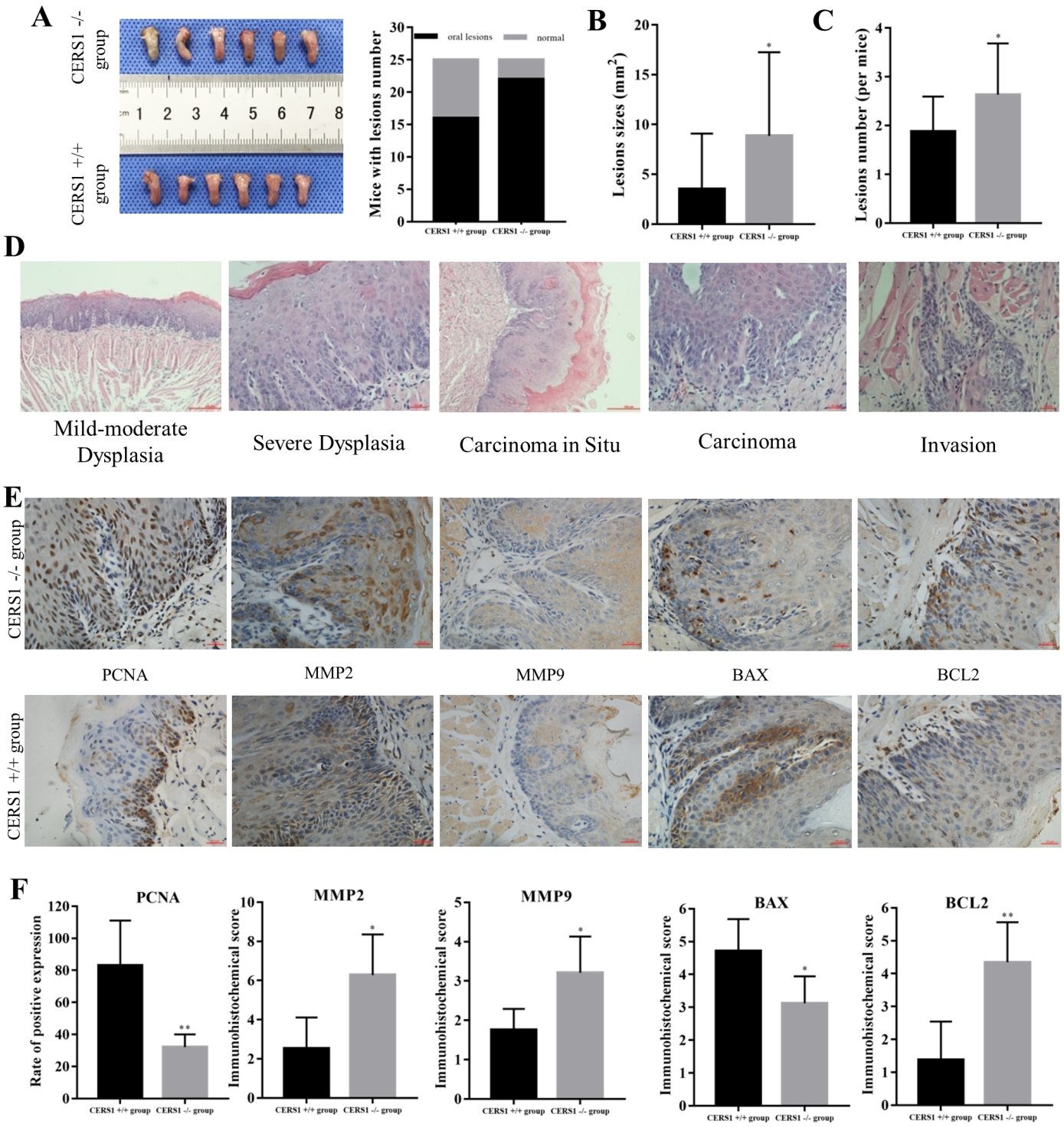

Figure 3

CERS1 knockout promoted OSCC occurrence in vivo. A to C, gross appearances of the tongue are shown. The number of mice with lesions (A), lesion sizes (B) lesion number per mouse (C) confirmed that CERS1 knockout promoted OSCC in vivo. D, pathological analysis of representative H&E sections show mild moderate dysplasia, severe dysplasia, carcinoma in situ, carcinoma and invasion. E and F,

immunohistochemical detection of hyperplastic lesions in tongue tissues. For D and E, magnifications were ×100 and ×400. For F, Student's t test was used. Note: *, p < 0.05; **, p < 0.01; ***, p < 0.001.

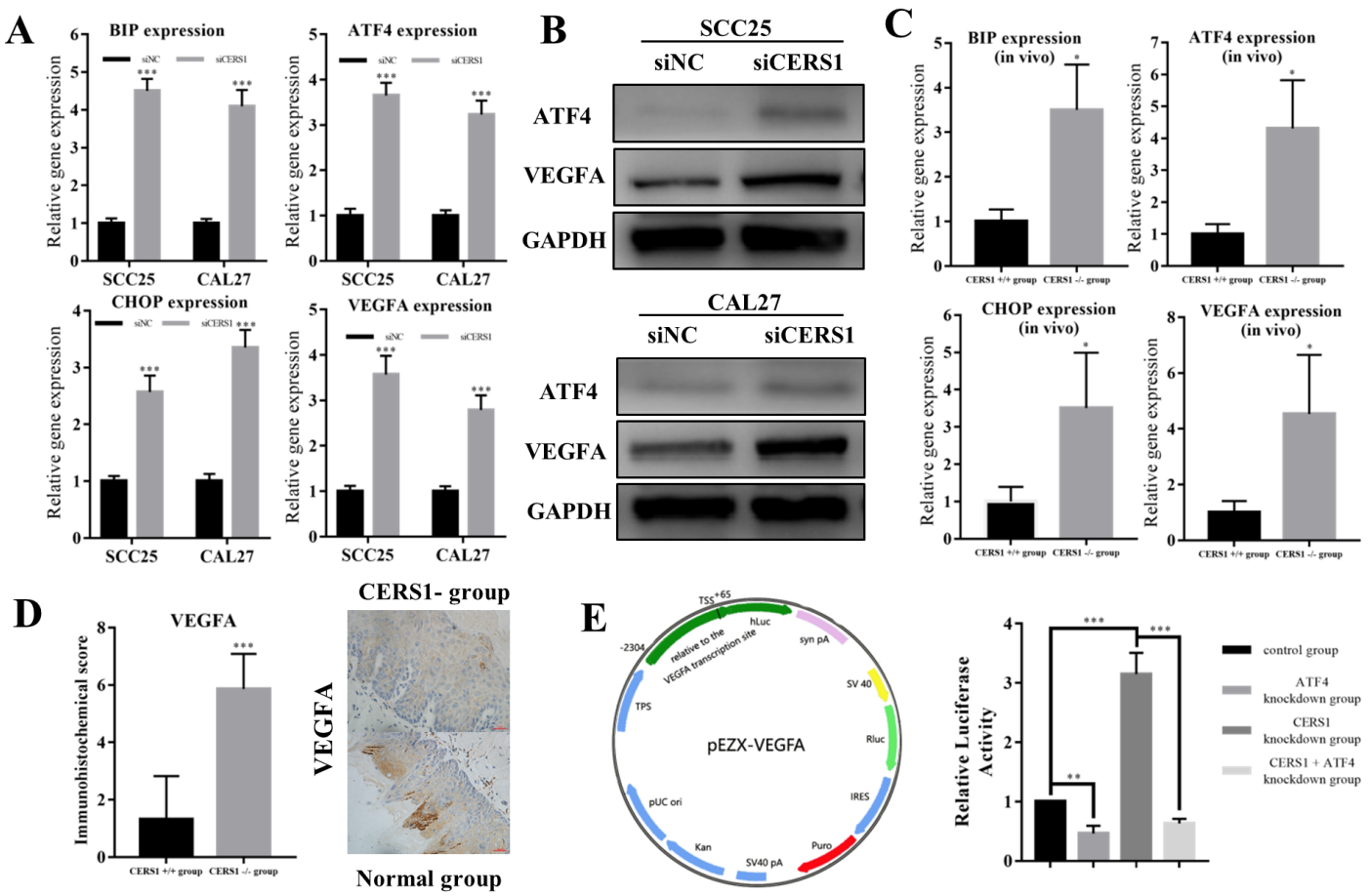

Figure 4

CERS1 knockdown induced ER stress, upregulating VEGFA. A to C, RT-PCR and Western blot analysis showed the expression of ER stress markers (BIP, CHOP, ATF4) and VEGFA in OSCC cells and in mice with tongue tissue lesions. D, immunohistochemical detection showed the expression of VEGFA in mice with tongue tissue lesions. E, the pEZX-VEGFA luciferase reporter plasmid constructs show the location of the insert (-2304 to +65 relative to the VEGFA transcription initiation site). After CERS1 knockdown, VEGFA promoter activity remained stable if ATF4 was downregulated. The RT-PCR results confirmed that CERS1 knockdown promoted VEGFA expression through ATF4 upregulation. For A, B, D and E, Student's t test was used. For D, magnifications were ×400. Note: *, p < 0.05; **, p < 0.01; ***, p < 0.001.

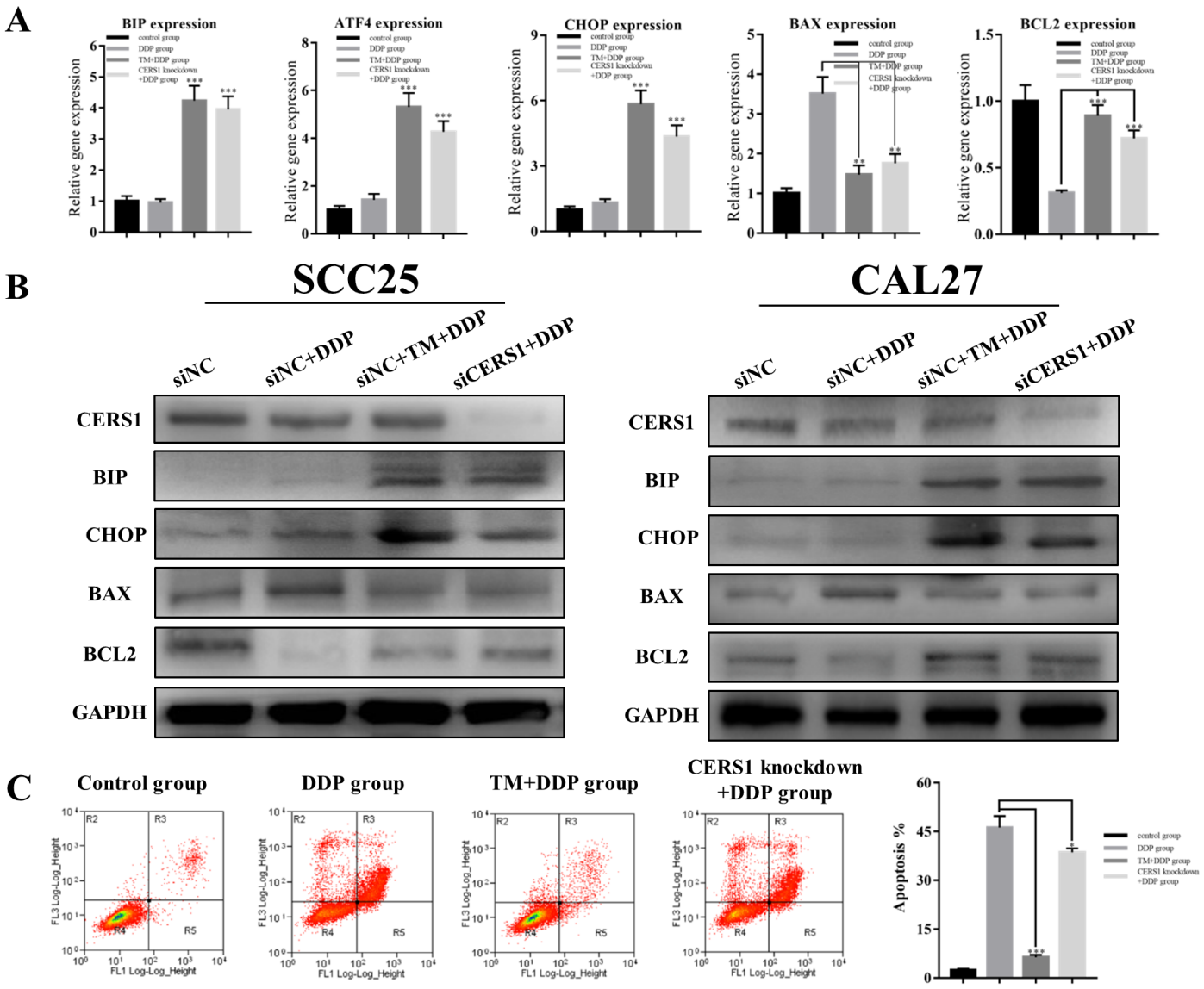

Figure 5

CERS1 knockdown regulated cisplatin resistance through mild ER stress. A and C, treatment with low-dose TM and CERS1 knockdown had the same impact on OSCC cells for cisplatin resistance, that is, by inducing mild ER stress (the expression of BIP and CHOP was mildly upregulated) and suppressing apoptosis (the expression of BAX and BCL2; Annexin V/PI double staining). For A to C, one-way ANOVA and Dunnett's t test were used, "Control group" was selected as the standard. Note: *, $p < 0.05$; **, $p < 0.01$; ***, $p < 0.001$.